DARWIN 1.5 : Large Language Models as Materials Science Adapted Learners

Tong Xie[1,2*†], Yuwei Wan[2,3†], Yixuan Liu[2], Yuchen Zeng[4], Wenjie Zhang[6], Chunyu Kit[3], Dongzhan Zhou[5*], Bram Hoex[1*]

[1*]School of Photovoltaic and Renewable Energy Engineering, University of New South Wales, Kensington, NSW, Australia.
[2]GreenDynamics, Sydney, NSW, Australia.
[3]Department of Linguistics and Translation, City University of Hong Kong, Hong Kong, China.
[4]Department of Computer Science, University of Wisconsin-Madison, Madison, Wisconsin, United States.
[5]Shanghai Artificial Intelligence Laboratory, Shanghai, China.
[6]School of Computer Science and Engineering, University of New South Wales, Kensington, NSW, Australia.

*Corresponding author(s). E-mail(s): tong@greendynamics.com.au; b.hoex@unsw.edu.au;
†These authors contributed equally to this work.

Abstract

Materials discovery and design aim to find components and structures with desirable properties over highly complex and diverse search spaces. Traditional solutions, such as high-throughput simulations and machine learning (ML), often rely on complex descriptors, which hinder generalizability and transferability across tasks. Moreover, these descriptors may deviate from experimental data due to inevitable defects and purity issues in the real world, which may reduce their effectiveness in practical applications. To address these challenges, we propose Darwin 1.5, an open-source large language model (LLM) tailored for materials science. By leveraging natural language as input, Darwin eliminates the need for task-specific descriptors and enables a flexible, unified approach to material property prediction and discovery. We employ a two-stage training strategy combining question-answering (QA) fine-tuning with multi-task learning (MTL) to inject domain-specific knowledge in various modality and facilitate cross-task knowledge transfer. Through our strategic approach, we achieved a significant

enhancement in the prediction accuracy of LLMs, with a maximum improvement of 60% compared to LLaMA-7B base models. It further outperforms traditional machine learning models on various tasks in material science, showcasing the potential of LLMs to provide a more versatile and scalable foundation model for materials discovery and design.

Keywords: Large language models, multi-task learning, property prediction

1 Introduction

Materials discovery and design aim to efficiently identify candidates with desired properties within a vast and complex space. This process faces challenges due to increasing structural and chemical diversity and complex structure-property-synthesis-performance relationships. The lack of a universal exploration method for the largely unlabeled materials data limits search efficiency. To address this, researchers employ two key approaches: (i) principle calculation, which provides accurate insights into material properties through high-throughput simulations, and (ii) machine learning (ML) techniques, which leverage growing materials datasets to expedite discovery workflows. Both strategies seek to navigate the complex materials landscape more efficiently, accelerating the discovery of new materials with targeted properties for various functional applications.

The adoption of ML in materials science faces significant challenges in developing universal input descriptors, primarily due to the disconnect between human-readable descriptions (e.g., "Tetragonal TiO2") and machine-readable formats required for ML models (e.g., TiO2 CIF file). This necessitates a complex translation process, often resulting in two key issues: (1) the creation of descriptors or features that lack generality, leading to poor transferability across different prediction tasks, and (2) overly complex model designs that further hinder broad applicability. Additionally, the heterogeneous nature of experimental materials, which often deviate from idealized material structures due to defects, impurities, or unique local environments, presents a significant obstacle. These real-world complexities are not easily captured by simplistic representations based on basic structural units, causing ML models to gauge the performance of experimental materials ineffectively. Consequently, there is a pressing need for a more sophisticated, flexible, and universal foundational model that can effectively bridge the gap between human understanding, computational models, and experimental realities while remaining adaptable across diverse prediction tasks and material classes.

Large language models (LLMs), represented by ChatGPT [1], have captivated the academic community due to their proficiency in understanding directives and generating responses akin to human conversation. Compared to traditional machine learning methods taking carefully designed descriptors as inputs, such as random forest [2], SVM [3], and Gaussian Process [4], LLMs can directly process human-readable descriptions, which avoids the need for designing special input formats required for each task.

Additionally, LLMs demonstrate potent generalization across various tasks, illustrating their capacity to resolve unseen or intricate challenges in natural science. [5, 6] are pioneering works in this direction, which demonstrate the efficacy of GPT models in solving chemical and material tasks, especially in the situation where available data are scarce, just as the wet-lab experimental scenarios. However, the core issue with these models lies in the fact that they remain inaccessible as open-source platforms, consequently compelling each user to engage in the laborious and financially burdensome task of individually fine-tuning the model on OpenAI's servers. Furthermore, they fail to offer a robust degree of confidence in their precision, which reduces the trustworthiness and transparency of the model and thus can be viewed as a significant shortfall. Such constraints have the potential to impose a brake on the momentum at which LLMs are propelling scientific discovery.

In this work, we propose Darwin 1.5, an open-source foundational LLM tailored for material science and chemistry. We design a two-stage training strategy, i.e., QA fine-tuning and multi-task learning to endow LLMs with the capability to proficiently perform these tasks. The QA dataset in the first stage is derived from highly-cited scientific literature, which not only facilitates the injection of critical 'know-how' knowledge into LLMs but also better emulates the paradigm by which human chemists or materials scientists perform tasks—by analyzing and interpreting literature, rather than exclusively relying on complex computational simulations such as operations involving CIF files. Different from [5] that finetunes separate LLMs for each task, we employ a multi-task learning mechanism in the second stage to perform different tasks simultaneously, which consists of 5 classification and 17 regression tasks closely related to the common properties of molecules and materials, spanning diverse systems. This mechanism effectively leverages the synergy between tasks and mitigates the imbalance problem among data distribution, enabling shared learning of underlying representations and cross-task knowledge transfer. We conduct extensive experiments to validate the effectiveness of our approach, which achieves on-par or even better performance comparable with machine learning models across various tasks. Most importantly, our study highlights the potential of large language models (LLMs) to internalize diverse types of data, paving the way toward the development of a universal model for chemistry and material science.

2 Results

Existing attempts to apply machine learning to material and chemistry typically rely on specially designed descriptors as inputs. Despite their effectiveness in various tasks, these descriptors may suffer from complex design and limited transferability across different tasks. Additionally, theoretical descriptors may exhibit discrepancies in experimental data. In contrast, our method leverages natural language as a carrier, which facilitates the unification of diverse tasks into a single input format and allows for the seamless incorporation of the 'know-how' information, thereby enhancing its applicability to experimental settings.

To improve the capability of LLMs, we incorporate the SciQAG-24D dataset [7], a question-answering (QA) dataset derived from scientific papers. The training set

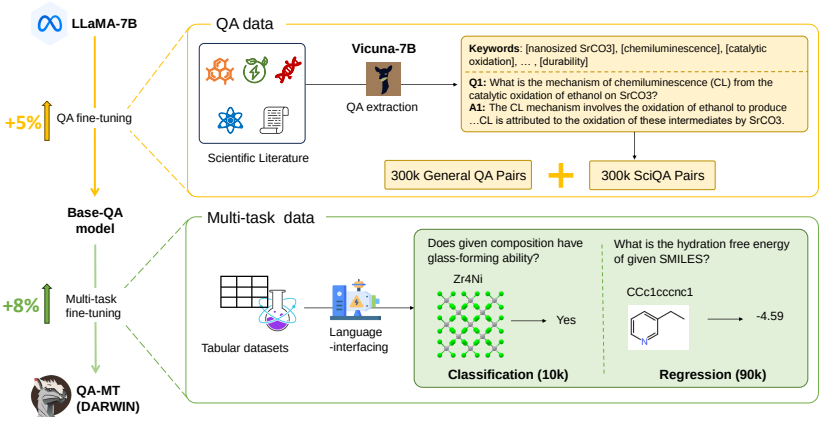

Fig. 1 Overview of Darwin. We adopt a two-stage training strategy, i.e., QA fine-tuning and multi-task learning, to achieve effective domain knowledge injection and enable the model to perform various core tasks in material and chemistry simultaneously.

consists of 28k open-ended QA pairs, preserving essential knowledge from lengthy scientific texts. This real-world data mitigates the risk of model collapse that may occur when training exclusively on LLM-generated content. Moreover, the QA task could enrich the model with specialized scientific expertise and thus raise its adaptation across various tasks.

Multi-task learning (MTL) is an approach where a model learns to perform multiple related tasks simultaneously by sharing representations, which helps improve its ability to generalize on each task [8]. MTL is particularly valuable in the context of material science as it can effectively capture the underlying commonalities across different yet correlated material properties, thereby improving performance for each task in deep learning [9]. In practice, Multi-Task Learning (MTL) tends to select identical representations for the single type of material inputs, such as SMILES for polymer [10], and trains on strongly related properties, such as Formation Energy (ΔE^f), Band Gap (E_g), and Fermi Energy (E^F) [9]. To investigate whether this holds when applied to LLMs, we transferred 5 classification tasks and 17 regression tasks from 21 datasets concerning common material properties, most of which have well-established machine learning baselines from previous research. The datasets covered diverse material systems from inorganics to composites, characterizing their fundamental physical, chemical, and electrochemical properties. Diverse material representations such as compositions, material names, SMILES notations, and structural motifs are used in the datasets. Classification tasks involve predicting discrete categories or labels, while regression tasks focus on predicting continuous numerical values of properties.

To harness the full potential of LLMs for materials science applications, it is necessary to convert original datasets into a language-interfaced format suitable for fine-tuning these models. Inspired by Language-Interfaced Fine-Tuning (LIFT) [11] and gptchem [5], we design a set of prompt templates to convert samples in the 21

datasets into natural language sentences. The original data, which consists of material names (or representations) and outputs, such as labels or numeric values, is integrated with natural language descriptions of feature names and task-specific prompts. This leads to instructions that combine inputs and expected outputs. For example, an instruction may look like: 'What is the band gap of given composition?' with input 'CdCu2SnS4', and our model should give a text output '1.37', which can be converted to a numeric value. To reduce hallucinations, we add 5% counterexamples in the training set of each task.

We explored the impact of QA and MTL fine-tuning on 22 task performance using the open-source LLaMA series [12]. Our experimental setups include 4 fine-tuning strategies:

1) Single-task: we fine-tune the LLMs using a training set of each specific task, which allows us to assess the models' ability to adapt to individual tasks and establish a baseline for a fair comparison. We obtain a fine-tuned model for each task in this setup, named 'Base-ST'.

2) Multi-task: we fine-tuned the LLMs using a mixture of all training datasets from 22 tasks. We obtained one fine-tuned model to perform all the tasks in this setup, named 'Base-MT'.

3) QA-single (2-stage): we fine-tune the LLMs first on QA data (named 'Base-QA'), then further fine-tune it using each specific task. In addition to the 'Base-QA' model, we obtain 22 fine-tuned models, denoted as 'QA-ST'.

4) QA-multi (2-stage): we fine-tune the 'Base-QA' model using a mixture of all training datasets from 22 tasks, denoted as 'QA-MT'.

2.1 Results of QA and multi-task fine-tuning

After fine-tuning the models, we evaluate their performance on the test data of each task separately (for each Base-ST and QA-ST model, we evaluate its performance on the corresponding test data). For classification tasks, we use the balanced macro F1-score, while for regression tasks, we employ mean absolute error (MAE). In Figure 2, we compare the task performance to figure out how different fine-tuning strategies influence the results. For classification tasks, QA fine-tuning leads to an average improvement of 1.55%, while multi-task fine-tuning results in an average improvement of 2.42%. The two-stage fine-tuning (QA-MT) achieves an average improvement of 2.82% compared to the Base-ST model. In regression tasks, QA fine-tuning yields an average improvement of 6.56%, while multi-task fine-tuning offers a significantly higher average improvement of 14.33%. Two-stage fine-tuning achieves the highest performance with a 15.52% improvement over the baseline. The results indicate that both QA fine-tuning and multi-task learning (MTL) strategies contribute positively to the performance of LLMs. When used together, these strategies effectively inject the 'know-how' knowledge and leverage the synergistic effects between tasks, further enhancing the model's capabilities.

In Figure 3, we compare the performance of QA-MT with competitive machine learning algorithms. The results indicate that QA-MT outperforms or achieves comparable results with the machine learning baselines (Methods) on most tasks,

demonstrating the effectiveness of our approach. Since our method directly takes natural language as input, it offers greater flexibility and is easier to implement compared to machine learning tasks that rely on complex data structures. Notable, when comparing with more advanced closed-source GPT series, QA-MT consistently surpasses both GPT-3.5 single-task fine-tuning and GPT-4 [13] few-shot prompting, which demonstrates the advantages of our method for handling diverse material science applications.

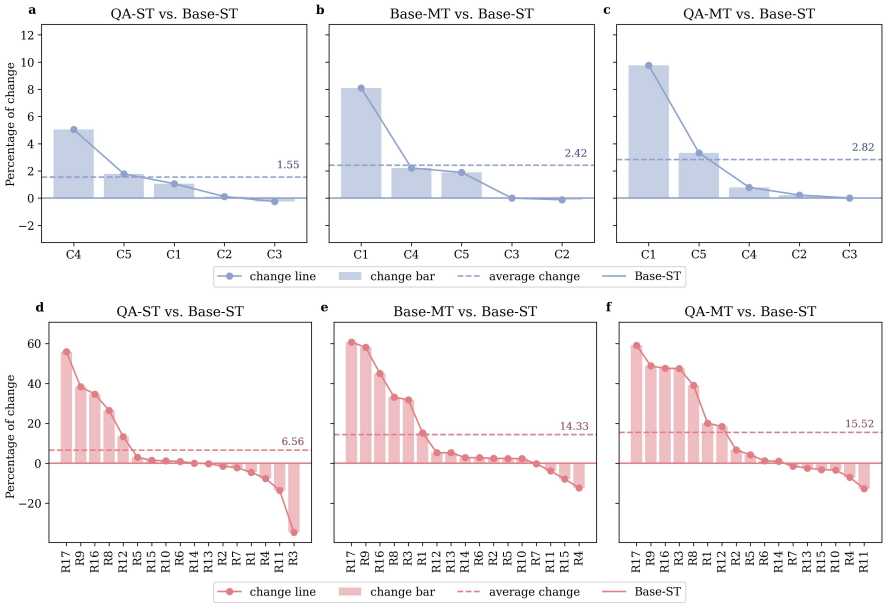

Fig. 2 Comparison of different fine-tuning strategies on task performance. Base-ST is used as baseline and bars illustrate the difference between models on the specific tasks. The average improvement is indicated by the dashed line.

In comparing the model performance after applying three fine-tuning strategies across different tasks, we observe a notable variation in improvement, particularly for regression tasks. For example, the most improved task R17 shows up to a 60% enhancement brought by multi-task fine-tuning; however, a few tasks, like R4 and R11, even experience a slight decrease in performance compared to the single-task baseline. Though our fine-tuning strategies yield significant overall improvements, the gains associated with each strategy are not evenly distributed across tasks. This phenomenon suggests that different tasks may have varying levels of compatibility with specific fine-tuning strategies, with some tasks showing a clear preference for a certain strategy. Based on these findings, we speculate that in multi-task fine-tuning, some tasks may be more effectively grouped together, while others may not, highlighting differences in inter-task relatedness.

As for specific tasks, classification task C1, C4, and C5 exhibits higher improvement while C2 and C3 shows less improvements. It should be noticed that C1 experiences

a 8% improvement in Base-MT, but only about 1% in QA-ST. The variability in performance gains resulting from different fine-tuning strategies is more pronounced in regression tasks. Though the distribution of performance improvements also shows similarities across different fine-tuning strategies, there are notable exceptions. For instance, multi-task fine-tuning reduced the MAE of R3 by approximately 30%, while QA fine-tuning did not improve R3 and even slightly worsened performance compared to the single-task baseline. This indirectly suggests that while QA and multi-task fine-tuning provide some common knowledge, they also emphasize different aspects.

Fig. 3 Comparison of model performance relative to QA-MT across tasks. Points on the left of the vertical line indicate poorer performance compared to QA-MT.

We have conducted further experiments to elucidate the mechanisms underlying the improved performance of LLM through 2-stage fine-tuning. In the following sections, we will provide a detailed analysis of the key factors driving this enhancement.

2.2 Evaluating the impact of pretraining on fine-tuning performance

We hypothesize that the general language capabilities acquired during the pretraining phase establish a robust foundation for subsequent QA fine-tuning and multi-task fine-tuning. To verify this, we conduct comparative experiments to assess the influence of pretraining in applying LLMs in material science. The fine-tuning strategies followed the same approaches as described earlier in (1) and (2), but with a key difference - we used an untrained LLaMA-7B model (with all parameters randomly initialized) as the base model. The single-task fine-tuning results in 22 specialized task models, referred to as "Random-ST" while the multi-task fine-tuning yields a single multi-task model, named "Random-MT".

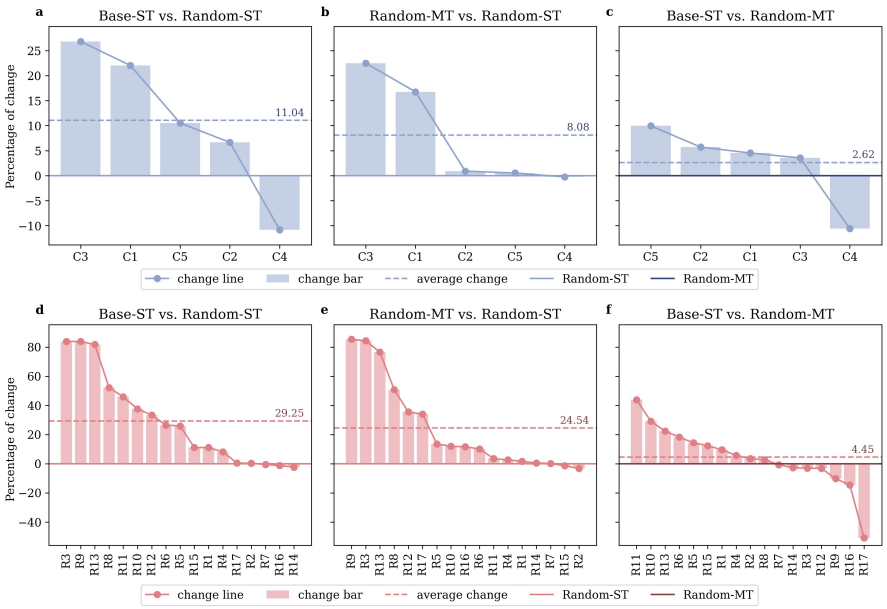

Fig. 4 Comparative Performance of Pretrained and Non-Pretrained Models under Single-Task and Multi-Task Fine-Tuning Strategies. **a, d**. Single-task fine-tuning results, comparing pretrained (Base-ST) and non-pretrained (Random-ST) models. **b, e**. Multi-task fine-tuning results for non-pretrained (Random-MT) versus single-task non-pretrained (Random-ST) models. **c, f**. Comparison of pretraining and multi-task fine-tuning effects on overall performance. **a, b, c** show results on classification tasks and **d,e,f** show results on regression tasks.

As shown in Figure 4, when using the Random-ST as the comparison benchmark, we observed that the pretrained model (Base-ST) achieved significantly better performance on single-task fine-tuning (Figure 4a & 4d): an average improvement of 11.04% on classification tasks and 29.25% on regression tasks. However, the gains from pretraining were not evenly distributed across tasks, suggesting that the background knowledge encoded during pretraining had varying degrees of relevance for different tasks.

Furthermore, by comparing Random-MT and Random-ST (Figure 2b & 2f), we could further examine the benefits of the multi-task fine-tuning strategy. Interestingly, the multi-task fine-tuning approach provided more remarkable improvements (up to 24.54% on regression tasks) on the non-pretrained model compared to the pretrained counterpart.

Comparing the gains from pretraining and multi-task fine-tuning (Figure 2c & 2g), we found that the latter could achieve near-equivalent performance to the former, albeit with slightly different emphases. This observation prompted further exploration of the distinct characteristics of these two approaches.

We hypothesize that the pretraining data contained a higher prevalence of more general material representations, such as material names and compositions, while more specialized expressions like SMILES and MOFs were less common. To investigate this,

we divided the 22 tasks into "general" (material names, compositions) and "specialized" (SMILES, MOFs) categories and compared the gains from pretraining and the different fine-tuning strategies. As shown in Figure 5, the pretraining-induced gains were more pronounced for the general category tasks, nearly double the specialized tasks. Similarly, the multi-task fine-tuning on the non-pretrained LLaMA model also benefited the general representation tasks more. However, when applied to the pretrained LLaMA model, this categorical difference was less pronounced, suggesting that the general language capabilities acquired during pretraining underpin the domain-specific knowledge, and that language-interfaced multi-task fine-tuning can effectively leverage the knowledge encoded in LLMs to integrate diverse material representations, ultimately expanding their utility in natural sciences.

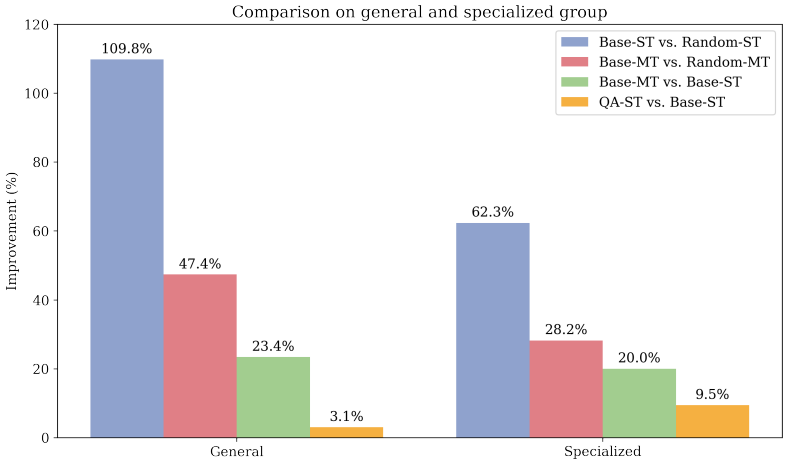

Fig. 5 Comparative gains of pretraining and fine-tuning on general and specialized material representation tasks. This figure compares performance gains from pretraining and subsequent fine-tuning across two task categories: general (e.g., material names and compositions) and specialized (e.g., SMILES, MOFs).

2.3 Investigate factors that improve prediction performance

Based on our observations from the preceding sections that multi-task fine-tuning demonstrated particularly significant improvements in regression tasks, we conducted detailed ablation studies using two widely recognized regression benchmark datasets from the materials science community: matbench_exp_bandgap and matbench_steel. To systematically investigate the mechanisms underlying the performance improvements, we designed multiple small-scale multi-task datasets by combining each target dataset with various auxiliary datasets:

Real dataset series:

1) +matbench: Incorporated three additional matbench tasks, all utilizing composition-based (General) material representations.

2) +other: Incorporated three tasks utilizing SMILES (specialized) representations, maintaining consistent total data volume.

Synthetic dataset series:

1) +Syn_1: Generated from three matbench tasks, maintaining original composition inputs but replacing property values with random numbers within the original min-max range (right name, fabricated value).

2) +Syn_2: Extended from +Syn_1, replacing material compositions with randomly generated alphabetical codes (e.g., "ABC") (both fabricated).

3) +Syn_3: Maintained original property values from the three matbench tasks but replaced material compositions with random alphabetical codes (fabricated name, right value).

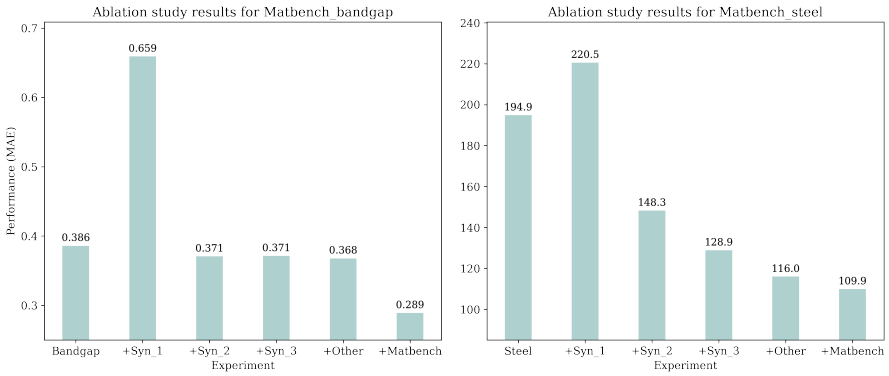

Fig. 6 Ablation study to understand mechanisms behind multi-task fine-tuning improvements. To investigate why multi-task fine-tuning enhances performance, we conducted an ablation study using carefully constructed auxiliary datasets. The datasets were designed to isolate the effects of instruction format, real knowledge and material representation types.

We fine-tuned multiple models on LLaMA-7B using these auxiliary datasets and evaluated their performance on the original test sets. As illustrated in Figure 6, all auxiliary datasets except +Syn_1 contributed to MAE reduction. Notably, the incorporation of incorrect property prediction data in +Syn_1 led to performance deterioration, increasing the bandgap MAE from 0.386 to 0.659. This degradation suggests that +Syn_1's incorrect property data introduces misleading knowledge that compromises model performance. The performance improvement observed with +Syn_2, despite its completely fabricated nature, demonstrates that model enhance its ability to correctly parse openended instructions and adhere to the specified requirements, which was defined as instruction-following ability [14], through pattern recognition in synthetic data structures. This finding suggests that the architectural benefits of multi-task learning persist even in the absence of meaningful domain knowledge. Exposure to a larger and more diverse set of training examples allows the model to better understand the nuances of the task and develop more robust and adaptable problem-solving strategies. The marginally superior performance of +Syn_3 compared

to +Syn_2 indicates that maintaining authentic property distributions, even with fabricated material inputs, allows the model to capture underlying statistical patterns in materials property relationships.

The impact of authentic auxiliary data proved particularly illuminating. Both +other and +matbench datasets demonstrated substantially greater performance improvements compared to their synthetic counterparts, underscoring the importance of genuine materials science knowledge in model training. The superior performance of +matbench over +other provides compelling evidence for the advantage of general composition representations in knowledge transfer. In the case of matbench_steel prediction, the reduction in MAE from 194.9 to 116.0 with +other, and to 109.9 with +matbench, representing an improvement of about 44% from the baseline performance. Comparing the performance improvements between +matbench and +Syn_2 enables us to decompose the overall benefits of multi-task fine-tuning: while +Syn_2 demonstrates the enhancement in instruction-following ability, the additional performance gains observed with +matbench can be attributed to the incorporation of domain-specific knowledge.

These observations corroborate our findings from the previous section: while LLMs can effectively learn and establish connections across specialized material representations through their general language capabilities and multi-task training, they demonstrate more comprehensive understanding and learning of materials expressed in general representations. These ablation experiments reveal that the success of multi-task fine-tuning extends beyond the model's enhanced instruction-following capabilities acquired from increased data exposure; it encompasses the understanding and acquisition of real-world knowledge. The pretraining phase of large language models serves as a fundamental bridge for connecting knowledge across different representational frameworks.

2.4 The application of QA-MT on bandgap prediction

The bandgap, a fundamental electronic property of materials, is the energy difference between the highest occupied molecular orbital (valence band) and the lowest unoccupied molecular orbital (conduction band). It plays a crucial role in determining a material's electrical and optical properties, making it a key parameter in fields like semiconductor research, photovoltaics, and electronics. For AI models in materials science, predicting bandgaps serves as a robust benchmark to evaluate their effectiveness and adaptability to domain-specific tasks. Accurate bandgap predictions can indicate a model's capability in capturing essential material properties.

We compare several simulation methods with our QA-MT model for bandgap prediction. The methods include:

1. PBE (Perdew–Burke–Ernzerhof): A widely-used density functional theory (DFT) method, known for being computationally efficient but often underestimating bandgaps due to limitations in handling electron-electron interactions.

2. HSE (Heyd–Scuseria–Ernzerhof): A hybrid functional approach that improves accuracy over PBE by incorporating a portion of exact exchange, though at a higher computational cost.

3. GWE (GW Approximation): A many-body perturbation theory approach that provides highly accurate bandgap predictions by accounting for electron-electron interactions more precisely.

4. AFLOWE: An automatic high-throughput computational framework that leverages DFT to predict various material properties, including bandgaps, focusing on efficiency and scalability.

5. SVR (Support Vector Regression): A machine learning model that uses training data to predict bandgaps, showing flexibility but potentially limited by the quality of the training dataset.

Table 1 displays the results from each method, including Mean Absolute Deviation (MAD) and Root Mean Squared Error (RMSE) compared to experimental bandgap values ($E_{g,\text{exp}}$).

Table 1 Comparison of simulation methods for bandgap prediction with QA-MT (DARWIN).

Compos.	Exp.	PBE	HSE	GWE	AFLOWE	SVR	QA-MT
GaN	3.2	1.62 (-49%)	3.14 (-2%)	3.32 (4%)	1.85 (-42%)	4.45 (39%)	2 (-38%)
CdTe	1.6	0.62 (-61%)	1.52 (-3%)	1.76 (12%)	0.67 (-57%)	1.43 (-9%)	1.08 (-33%)
LiF	14.2	9.2 (-35%)	11.47 (-19%)	15.1 (6%)	8.27 (-42%)	9.87 (-30%)	11.7 (-18%)
TiO2	3.42	2.13 (-37%)	3.67 (7%)	3.73 (9%)	2.09 (-38%)	3.99 (16%)	3.3 (-4%)
CuSbS2	1.38	0.9 (-35%)	1.69 (22%)	1.1 (-20%)	0.79 (-42%)	1.39 (1%)	1.38 (0%)
ZnS	3.91	2.07 (-47%)	3.49 (-11%)	4.15 (6%)	2.6 (-33%)	3.12 (-20%)	2.9 (-26%)
Cu2ZnSnS4	1.6	0.28 (-83%)	0.09 (-94%)	1.64 (3%)	N/A	1.75 (9%)	1.46 (-8.8%)
PbTe	0.19	0 (-100%)	0.19 (0%)	0.26 (36%)	0 (-100%)	0.2 (5%)	0.3 (58%)
GaAs	1.52	0.19 (-86%)	1.12 (-26%)	1.52 (0%)	0.24 (-84%)	1.28 (-15%)	1.18 (-22%)
ZnO	3.44	0.67 (-81%)	2.49 (-28%)	3.2 (-7%)	1.87 (-46%)	3.41 (-1%)	3.2 (-7.0%)
MAD		1.65	0.67	0.22	1.6	0.75	0.72
RMSE		2.1	1	0.33	2.25	1.46	0.69

When examining the table, QA-MT achieves a MAD of 0.72 and an RMSE of 0.686. These values are competitive, indicating that QA-MT performs well in predicting

bandgap compared to traditional simulation methods. Specifically, QA-MT's MAD and RMSE are comparable to the best-performing methods, only slightly worse than GWE, which has the lowest MAD (0.22) and RMSE (0.33). This shows that our model, while not reaching GWE's accuracy, performs significantly better than other methods like PBE and AFLOWE. As for stability, QA-MT's results show a level between the HSE and SVR methods. While it outperforms HSE and SVR in certain cases, some predictions have relatively high errors, suggesting room for improvement in model robustness across different material types.

In conclusion, QA-MT demonstrates strong predictive capability for bandgaps, showcasing the potential of advanced language models in materials science. While it trails slightly behind GWE in terms of absolute accuracy, QA-MT offers several advantages that make it a valuable alternative with broader applicability across tasks. One key advantage is inference speed. Unlike traditional simulation methods, which are computationally intensive and can take hours or even days for complex materials, QA-MT can predict bandgaps almost instantly. This rapid inference makes it highly practical for high-throughput screening of materials, enabling researchers to explore large chemical spaces more efficiently. Another significant advantage of QA-MT is its minimal input requirements. Whereas methods like DFT-based simulations require detailed structural information about the material (such as atomic positions and lattice parameters), QA-MT only needs the material composition as input. In this study, we used only the composition of each material (e.g., "GaN" or "CdTe") to make predictions, without any additional structural details. This low barrier to input data allows QA-MT to be easily applied in scenarios where structural data may be incomplete, costly, or unavailable. Overall, QA-MT's combination of speed, minimal input requirements, and competitive accuracy positions it as a powerful tool for materials property prediction. Although improvements in stability are needed to reach the level of methods like GWE, QA-MT's strengths highlight the growing role of language models as a versatile and efficient alternative to traditional simulation-based approaches in materials science.

3 Conclusion

In this study, we probed the capability of large language models (LLMs) to predict material properties using various fine-tuning strategies, including single-task, multi-task, QA-single, and QA-multi (2-stage) approaches. We found that:

(1) The QA-multi (2-stage) strategy, which involves initial training on QA data followed by multi-task data, outperformed other fine-tuning methods. Using this strategy, the QA-MT model demonstrated superior material property prediction performance compared to GPT-3.5 single-task fine-tuning and GPT-4 prompting. It achieved results comparable to traditional machine learning models and even surpassed them in some tasks, achieving state-of-the-art (SOTA) performance, such as in experimental bandgap prediction.

(2) The general linguistic capabilities of pre-trained LLMs facilitate better learning of material knowledge during fine-tuning, enabling the recognition of underlying

patterns. However, this advantage is unevenly distributed, favoring tasks that involve more general material expressions.

(3) Multi-task fine-tuning alleviates the imbalance mentioned in (2). This training strategy effectively leverages the knowledge encoded in LLMs to integrate diverse material representations, ultimately improving performance across different material representation tasks.

(4) In addition to enhancing instruction-following abilities through exposure to larger datasets, multi-task fine-tuning enables LLMs to autonomously distill implicit material knowledge from real-world data, even when such data is only tangentially related. This fosters a deeper understanding of materials and their properties.

The success of two-stage fine-tuning presents significant implications for future research. LLMs trained on vast natural language corpora excel at identifying contexts, patterns, and meanings, while uncovering hidden connections across diverse types of information. This makes them particularly suited for bridging and managing complex, heterogeneous representations. The ability to synthesize these varied representations enables LLMs to 1) identify subtle patterns in materials behavior; 2) connect processing parameters with resultant properties; 3) bridge theoretical predictions and experimental observations; 4) integrate multiscale phenomena, from atomic to macroscopic levels. In scientific literature, knowledge spans theoretical principles, experimental insights, material properties and characteristics, as well as structural information. In this study, we fine-tuned LLMs using material-related QA datasets to enhance their understanding of the materials domain. By learning to comprehend and reason about material-related questions and answers, the model can acquire a deeper grasp of the relevant scientific concepts and their implications. However, an alternative approach worth exploring involves conducting continued pretraining with a carefully balanced mix of general-text and materials science literature. Furthermore, given the relatively sparse representation of specialized notations such as SMILES in natural language-based scientific documents, a practical solution is to gather more real-world data with similar expressions for large-scale multi-task fine-tuning. Another promising avenue is incorporating targeted learning of specialized expressions during continued pretraining.

In summary, the synergistic combination of pretrained model properties, multi-task fine-tuning, QA-induced background knowledge, and increased data volume collectively contribute to the improved performance of the material property prediction task. our findings underscore the importance of multi-task learning in optimizing large language models for diverse and complex problem spaces. By training on multiple tasks simultaneously, models not only achieve superior performance but also uncover important connections between tasks, which enhances their ability to generalize. This approach holds promise for advancing AI-driven solutions across a variety of fields, offering a pathway to more robust and adaptable models capable of tackling a broad spectrum of challenges.

4 Methods

4.1 Datasets

FAIR stands for 'Findable, Accessible, Interoperable, and Reusable', which is a set of principles for enhancing the value and accessibility of data [15]. Due to the strong impact of 4V (volume, variety, velocity, and veracity) of Big Data on materials science, efforts have been made in recent years to collect comprehensive data from research groups worldwide, including unpublished data, and ensure its FAIRness [16]. We collected 21 open-accessed FAIR datasets from highly cited publications in materials science. The details of these datasets and which tasks they are used to derive instructions can be found in Appendix Table A.

The classification task of scientific language models involves the categorization or labelling of scientific text data into predefined classes or categories. For example, LLM can be trained to classify chemical compounds based on their properties, such as solubility, toxicity, or stability. This can assist in drug discovery, material science, or chemical engineering applications. A more demanding task than classification involves developing a regression model capable of predicting continuous property values. We design several prompt templates B to convert samples in the 21 datasets into natural language sentences.

4.2 Artificial counterexamples

One prevalent issue with LLMs is the generation of hallucinations—incorrect or fabricated information presented as factual [17]. To address this, we explored the effectiveness of incorporating artificial counterexamples into the fine-tuning process of LLMs. Our hypothesis is that by exposing the model to deliberately incorrect information during training, the model learns to distinguish between factual data and potential hallucinations. This pilot study was designed to address several research questions: 1) Does the inclusion of counterexamples in the fine-tuning process reduce the occurrence of hallucinations? 2) Does the integration of counterexamples during training negatively impact the model's performance on the normal test set? 3) Is there a correlation between the proportion of counterexamples included in training and the reduction of hallucinations?

To answer above questions, we selected x classification tasks, x regression tasks that require the model to generate or infer detailed scientific information, such as predicting whether a composition is glass. Due to adherence to the format during fine-tuning, the model tends to predict whether nearly all inputs using format trained. For example, it predicts 'farmer' as FALSE (not glass), even though 'farmer' is not even a composition. This is clearly inconsistent with the facts. For each task selected, we created artificial counterexamples which involve intentionally providing incorrect or irrelevant inputs that don't match the expected types (see Data in Methods section). We then fine-tuned the model with varying ratios of these counterexamples integrated into the 500 training samples, specifically 0% (baseline), 1%, 2%, 5%, 10% and 20% of the total training data. The evaluation had two stages: First, we assessed the model's performance on a 100-sample test set without fabrications, recording metrics like MAE

and F1-score to see if counterexamples affected its primary function. Second, we tested with 100 artificial counterexamples to evaluate the model's accuracy in identifying and handling hallucinations, focusing on rejecting false information and maintaining output integrity.

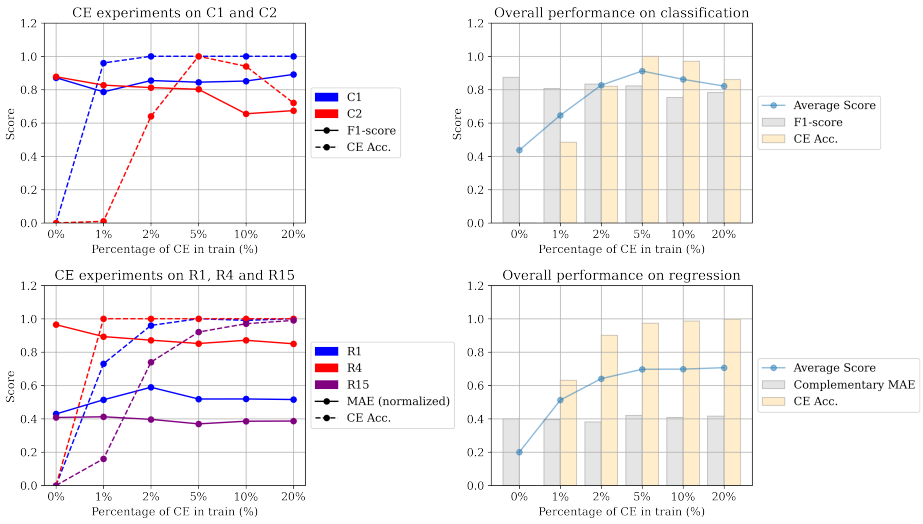

Fig. 7 Results of counterexample experiments.

As shown in Figure 7, the results indicate that incorporating counterexamples into the training procedure effectively reduces hallucinations. Models trained with counterexamples exhibited a marked decrease in the generation of incorrect information during the counterexample test evaluation. For instance, with a 5% ratio of counterexamples, hallucinations were reduced by approximately 100% compared to the baseline. Importantly, the inclusion of counterexamples did not significantly impair the model's performance on normal test evaluations, with metrics such as MAE and F1-score remaining stable across small counterexample ratios. This suggests that the model can learn to identify and reject false information without compromising its ability to process and generate accurate data for standard tasks. Thus, for most machine learning training data in this study, we generated 5% counterexamples and mixed them with the original dataset. By fine-tuning models with a carefully balanced dataset that includes both normal and 'noisy' examples, we can enhance the reliability of these models in producing factual and trustworthy outputs.

4.3 Machine learning baselines

We included results from several machine learning models as references, like CrabNet, MODNet (v0.1.1), and AMMExpress v2020 from matbench [18] and machine learning baseline algorithm used in GPTchem [5]. It should be noted that each model was individually trained on a specific FAIR dataset. The detail results of these datasets and

which tasks they are used to derive instructions can be found in Appendix Table C. It is important to note that due to different representation formats of the input, not all tasks have machine learning baselines, and even if they do, they may not cover all types of baselines.

4.4 Fine-tuning strategy

For all QA-generator model, QA-base model and ST/MT models, We fine-tune the LLaMA models following established methods, using a setup of 4×AMD MI250X GPUs and employing the Brain Floating Point 16 (BF16) data format for an optimal balance between precision and computational efficiency. For the `LLaMA-3-8B-16k` model, which is for QA generation, we adopt the LongLoRA [19] method with Flash-Attention2 [20] and DeepSpeed stage 3 [21]. Training is conducted for 5 epochs with a per-device batch size of 1, maximum sequence length of 16,000, and gradient accumulation over 8 steps. The learning rate is set to 2e-5 with no weight decay, and warm-up steps are set to 20. For inference, we use a temperature of 0.6 and top_p of 0.9 for logical and diverse text generation.

Similarly, for QA-base model and MT model, the `LLaMA-7b` model is fine-tuned based on Stanford's Alpaca approach. DeepSpeed stage 2 [21] is employed with a batch size of 2 per device, maximum sequence length of 512, and gradient accumulation over 4 steps. The learning rate remains 2e-5 with no weight decay, while a warm-up ratio of 0.03 is applied. These configurations are tailored to handle the shorter question-answer (QA) and task sequences efficiently.

Due to the large volume of QA samples, we train for 3 epochs to avoid overfitting, with training completion in approximately 15 hours. For fine-tuning on single- and multi-task datasets, we increase the training to 5 epochs, with multi-task fine-tuning taking about 4 hours to complete. During inference, we set the temperature to 0.8 and top_p to 0.75, which makes text generated more logical with rich vocabulary.

In experiments involving the `gpt-series` models, we use `gpt-3.5-turbo-0613` for fine-tuning and `gpt-4-0613` for few-shot learning. For training, we utilize default parameters determined algorithmically by Azure OpenAI based on the size of the training data. During inference, we set the temperature to 0.8 to enhance generation diversity.

Declarations

Funding

This research was supported by generous funding and resources from multiple organizations. We gratefully acknowledge the support of: 1) The Australian Supercomputing Facility, which provided critical computational resources essential to our research infrastructure. 2) Microsoft Corporation, whose technological support and computational resources were instrumental in advancing our project. 3) The Australian Renewable Energy Agency (ARENA), whose financial support and commitment

to innovative energy research made this work possible. 4) The Australian Centre for Advanced Photovoltaics (ACAP), whose funding and scientific collaboration significantly contributed to our research outcomes.

We extend our sincere thanks to these organizations for their crucial support in enabling this research endeavor.

Competing interests

The authors declare no competing interests.

Ethics approval and consent to participate

Not applicable

Consent for publication

Not applicable

Materials availability

Not applicable

Data availability

The multi-task fine-tuning datasets used in this study, including training sets, test sets, small-scale multi-task datasets (subsection 2.3) are available via Figshare at 10.6084/m9.figshare.28023626. The weights of QA-MT model are provided in the Onedrive link in https://github.com/MasterAI-EAM/Darwin.

Code availability

The source code is freely available at https://github.com/MasterAI-EAM/Darwin under an MIT license. The versions of the packages used in the study are provided in the requirements file in GitHub repository.

Appendix A Details of datasets

Table A1: Details of FAIR datasets and associated tasks they are used to derive instructions, (R for regression; C for classification)

Dataset	Description	Task Code
`Matbench_is_metal` [18]	This dataset is retrieved from Zhuo et al.'s work, containing data on classifying metallicity from composition for 4921 chemical formulas.	C1

Matbench_glass [22]	This dataset is retrieved from a volume of the Landolt– Börnstein collection 'Nonequilibrium phase diagrams of ternary amorphous alloys', containing data on full bulk metallic glass formation ability for 5680 chemical formulas.	C2
Pei [23]	The dataset consists of 1252 observations with 625 single-phase and 627 multi-phase alloys, covering binaries and multi-component systems. We constructed a binary classification task on phase of alloys.	C3
WaterStability [24]	The dataset consists of water stabilities for over 200 MOFs (metal–organic frameworks), alongside a comprehensive set of chemical features encompassing the metal node, organic ligand, and metal-ligand molar ratios. We constructed 170 pairs of formula and its stability (high or low) from training set.	C4
UV [25]	This dataset includes 18,309 records of experimentally determined UV/vis absorption maxima, and associated extinction coefficients. We constructed a subset of 5,158 SMILES with absorption region classification (ultraviolet or visible).	C5
NagasawaOPV [26]	1203 experimental parameters of organic photovoltaic (OPV) materials are manually collected from the literature and subjected to machine learning with digitized chemical structures. We constructed 3 regression tasks by using SMILES to predict bandgap, highest occupied molecular orbital (HOMO) and polydispersity index (PDI)	R1, R2
Matbench_steels [18]	This dataset is retrieved from Citrine informatics, containing data on steel yield strengths from composition for 312 chemical formulas	R3
ChEMBL [27]	This dataset is sourced from a curated database of bioactive molecules with drug-like properties, focusing on the lipophilicity of 1899 molecular compounds in pharmacokinetics. The water-octanol partition coefficient (logD) is used to describe lipophilicity.	R4

MoosaviDiversity [28]	A diverse set of structures based on the chemical and geometric descriptors CH4, CO2. We constructed 5941 samples of SMILES and log Henry's Law constant for CH4 and CO2 using experimental part, which is actually from CoRE-2019 [29].	R5, R6
MoosaviCp [30]	Dataset for predicting the heat capacity of materials based on density functional theory simulations	R7
FreeSolv [31]	This dataset provides experimental and calculated hydration free energies for small molecules in water, along with experimental values and input files. We constructed 641 samples of SMILES and its hydration free energy.	R8
photoswitch [32]	The dataset includes experimentally-determined properties for 405 photoswitches. We constructed a regression task to predict E isomer transition wavelength of given SMILES.	R9
SuperCon_ML [33]	This work considers over 16,000 different compositions from SuperCon [34] database for machine learning. It houses information such as the critical temperature (Tc) and reporting journal publication for superconducting materials known from experiment. We extracted a list of 10,436 compounds with Tc reported.	R10
UCSB+ESTM [35, 36]	UCSB is a database of about 1,100 experimental thermoelectric materials from UCSB aggregated from 108 source publications and personal communications. ESTM is a public database of thermoelectric materials and system-identified material representation for data-driven discovery. We made a combination and cleaning of UCSB and ESTM to predict thermoelectric figure of merit (zT) of 5747 composition with temperature conditions.	R11

TADF [37]	A database of thermally activated delayed fuorescent (TADF) molecules was automatically generated from the scientifc literature. Among these, 5,349 records have chemical names in the form of SMILES strings which are represented with 91% accuracy. We constructed delayed lifetime (435 samples), emission wavelength (937 samples), and photoluminescence quantum yield (719 samples) of SMILES.	R12, R13, R14
Refractive [38]	The database comprises a total of 49,076 refractive index and 60,804 dielectric constant data records on 11,054 unique chemicals. We constructed 6,262 pairs of compound and its refractive index.	R15
Matbench_expt_gap [39]	This dataset is retrieved from Zhuo et al.'s work, containing data on experimental band gaps and DFT calculated zero band gaps for 4604 compounds.	R16
Seminconductor [40]	This work presents an auto-generated database of 100,236 semiconductor band gap records, extracted from 128,776 journal articles with their associated temperature information. We constructed 5,000 samples of material name and its averaged bandgap.	R16
QMUG [41]	The QMUG collection comprises quantum mechanical properties of more than 665 k biologically and pharmacologically relevant molecules. We constructed 6592 samples of SMILES and its HOMO-LUMO gap.	R16
ESOL [42]	This dataset is a compilation of measured aqueous solubility (LogS) values, a crucial factor in drug discovery. The dataset comprises 927 molecular compounds originally used for ESOL - estimated solubility.	R17
solubility [43]	A set of 100 molecules with measured and reported intrinsic aqueous solubilities, together with a suggested 75-25 training-test split.	R17

Appendix B Templates for converting tabular data to sentences

Label definition

<material_type>: The specific format (e.g. composition) used to represent a material's characteristics or structure.

<material_representation>: The actual representation of material (e.g. TiO2), typically showing its elemental composition or structural details.

<yes_no>: A binary response indicating the presence or absence of a specific characteristic. The format typically follows the pattern "Yes/No".

<has_>: A linguistic marker that indicates the presence or absence of a specific material property or characteristic, typically used to explicitly state whether a material possesses a particular attribute. It connects the material representation with a specific property in a grammatically complete statement. The format typically follows the pattern "has/have/does not have".

<property>: A characteristic or attribute (e.g. bandgap) of a material that describes its behavior, performance, or physical characteristics.

<property_value>: The numerical or quantitative measurement of a specific property of the material.

- **Classification templates**

Template 1:
Instruction: Tell me if given <material_type> <has_> <property>.
Input: <material_representation>
Output: <yes_no>, <material_representation> <has_> <property>.

Template 2:
Instruction: Does given <material_type> <has_> <property>?
Input: <material_representation>
Output: <yes_no>, <material_representation> <has_> <property>.

- **Regression templates**

Template 1:
Instruction: Given a <material_type>, write its <property>.
Input: <material_representation>
Output: <property_value>.

Template 2:
Instruction: Predict the <property> of this given <material_type>.
Input: <material_representation>
Output: <property_value>.

Template 3:
Instruction: What is the `<property>` of this given `<material_type>`?
Input: `<material_representation>`
Output: `<property_value>`.

Note: The above templates are applicable to data conversion for most tasks, with individual tasks having some adjustments. Please refer to the following examples for specifics.

- **Classification tasks**

C1 data example:
Instruction: Tell me if this composition is a metal.
Input: BaAg2
Output: Yes, BaAg2 is a metal.

C2 data example:
Instruction: Tell me if given composition has glass formation ability.
Input: Cr23Ni17Mo10
Output: Yes, Cr23Ni17Mo10 has glass formation ability.

C3 data example:
Instruction: Predict the phase of this given alloy.
Input: Al1Co1Cr1Cu1Fe1Mo0.4Ni1
Output: multi-phase

C4 data example:
Instruction: Predict the water stability of this given activated formula unit.
Input: Cr(OH)1,4-benzenedicarboxylate
Output: high

C5 data example:
Instruction: Given this SMILES, predict whether the compound would absorb light in the ultraviolet region or the visible region?
Input: Cr(OH)1,4-benzenedicarboxylate
Output: high

- **Regression tasks**

R1 data example:
Instruction: Predict the highest occupied molecular orbital (HOMO) of this given SMILES.

Input: CC1=CC2=C(C(SC(C3=CC=C(C)C4=NSN=C43)=C5)=C5N2C(CCCCC)CCCCC)S1
Output: 4.81

R2 data example:
Instruction: What is the poly dispersity index (PDI) of this given SMILES?
Input: CC(S1)=CC2=C1C(OCCCCCCCCCCCCC)=C(C=C(C3=C4C(OCCO4)=C(C)S3)S5)C5=C2OCCCCCCCCCCCC
Output: 1.9

R3 data example:
Instruction: Given a composition, write its yield strength.
Input: Fe0.768C0.000931Mn0.00244Si0.00199Cr0.110Ni0.0981Mo0.0113V0.000110Nb0.0000602Co0.0000948Al0.00497Ti0.00269
Output: 1167.2

R4 data example:
Instruction: What is the lipophilicity of given SMILES?
Input: CC(C)OC(=O)N1CCC(CC1)Oc2ncnc(Oc3ccc(cc3F)S(=O)(=O)C)c2C
Output: 3.54

R5 data example:
Instruction: Predict the the log Henry's Law constant for CO2 of given SMILES.
Input: [Co].c1ccc(cn1)[CH][N][N][CH]c1cccnc1
Output: -1.726468633

R6 data example:
Instruction: What is the the log Henry's Law constant for CH4 of given SMILES?
Input: N#Cc1cccc(c1)CN1CCN(CC1)Cc1cccc(c1)C#N.[Ag]
Output: -4.259713121

R7 data example:
Instruction: What is the gravimetric heat capacity at 300 K of this MOF with given features and topology?
Input: linker [O-]C(=O)c1cc([O])c(cc1[O])C(=O)[O-], nodes [Ni], topology pcu
Output: 15.84091337

R8 data example:
Instruction: Given this SMILES, write its hydration free energy.

Input: c1ccc(cc1)c2ccccc2
Output: -2.7

R9 data example:
Instruction: Predict the E isomer transition wavelength of given SMILES.
Input: CC(N(C)C(C)=C1C)=C1/N=N/C2=CC=CC=C2
Output: 345.0

R10 data example:
Instruction: Predict the critical termperature Tc in Kelvin K for a given superconductor composition.
Input: Ni2.5Cu1.5Zr8
Output: 1.09

R11 data example:
Instruction: Given composition with temperature conditions, write its thermoelectric figure of merit (zT).
Input: composition: Ti0.99Nb0.01NiSn, temperature (K):400.0
Output: 0.203822375

R12 data example:
Instruction: What is the photoluminescence quantum yield (%) of given SMILES?
Input: O=C1c2ccccc2C(=O)c2cc(Sc3ccc(-n4c5ccccc5c5ccccc54)cc3)ccc21
Output: 1.8

R13 data example:
Instruction: Given this SMILES, write its maximum emission wavelength (nm).
Input: c1ccc2c(c1)nc1n(-c3ccc(-c4ccc5oc6ccccc6c5c4)cn3)c3ccccc3n21
Output: 483.0

R14 data example:
Instruction: What is the delayed lifetime (µs) of given SMILES?
Input: O=C(c1ccc(N2c3ccccc3Oc3ccccc32)cc1)c1cccc(C(=O)c2ccc(N3c4ccccc4Oc4ccccc43)cc2)n1
Output: 1.0

R15 data example:
Instruction: Given this compound, write its averaged refractive index.
Input: CsNO3
Output: 1.3479

R16 data example:
Instruction: What is the averaged band gap of given material?
Input: heptazine
Output: 2.7

R17 data example:
Instruction: Given a SMILES, write its water solubility expressed as a logarithm in mol/L.
Input: c1cc2ccc3cccc4c3c2c(c1)cc4
Output: -6.18

Appendix C Machine learning results

Table C2: Results of machine learning baselines

Task	GPTchem	CrabNet	Others
C1		0.961	0.92
C2		0.909	0.9787
C3			0.93
C4			0.86
C5			
R1	0.11		1.67
R2	0.857		1.414
R3		182.9405	
R4	1.024		0.6706
R5	0.5622		0.51
R6	0.2412		0.2
R7			
R8	0.623		1.35
R9	10.286		25
R10			
R11			
R12	23.7133		
R13	46.332		
R14	1290.667		
R15			
R16			
R17			

Appendix D LoRA Results

Table D3: Results of LoRA Fine-Tuning on Each FAIR Task

Task	LlaMA-ST	QA-ST
C1	0.4682	0.6567
C2	0.726	0.8365
C3	0.3333	0.4
C4	0.4	0.898
C5	0.1932	0.6672
R1	0.3466	7.2155
R2	1.3111	1.414
R3	1566.5858	1187.3564
R4	1.4021	3.0897
R5	3.7006	5.4472
R6	1.34	8.7431
R7	6.0984	255.4198
R8	5.0269	62.7915
R9	328.4036	316.985
R10	15.4674	22.5444
R11	0.3712	17.4563
R12	34.5563	48.3285
R13	105.1862	189.57778
R14	429.3761	147.708
R15	1.3875	2.1887
R16	0.7663	7.1009
R17	2.6799	8.9210

References

[1] OpenAI: GPT-4 Technical Report. Preprint at https://arxiv.org/abs/2303.08774 (2023)

[2] Breiman, L.: Random forests. Machine learning **45**, 5–32 (2001)

[3] Cortes, C.: Support-vector networks. Machine Learning (1995)

[4] Rasmussen, C.E.: Gaussian processes in machine learning. In: Summer School on Machine Learning, pp. 63–71. Springer, ??? (2003)

[5] Jablonka, K.M., Schwaller, P., Ortega-Guerrero, A., Smit, B.: Leveraging large language models for predictive chemistry. Nature Machine Intelligence **6**(2), 161–169 (2024)

[6] Xie, T., Wan, Y., Zhou, Y., Huang, W., Liu, Y., Linghu, Q., Wang, S., Kit, C., Grazian, C., Zhang, W., et al.: Creation of a structured solar cell material dataset and performance prediction using large language models. Patterns **5**(5) (2024)

[7] Wan, Y., Ajith, A., Liu, Y., Lu, K., Grazian, C., Hoex, B., Zhang, W., Kit, C., Xie, T., Foster, I.: SciQAG: A Framework for Auto-Generated Scientific Question Answering Dataset with Fine-grained Evaluation. Preprint at https://arxiv.org/abs/2405.09939 (2024)

[8] Ruder, S.: An Overview of Multi-Task Learning in Deep Neural Networks. Preprint at https://arxiv.org/abs/1706.05098 (2017)

[9] Sanyal, S., Balachandran, J., Yadati, N., Kumar, A., Rajagopalan, P., Sanyal, S., Talukdar, P.: Mt-cgcnn: Integrating crystal graph convolutional neural network with multitask learning for material property prediction. Preprint at https://arxiv.org/abs/1811.05660 (2018)

[10] Kuenneth, C., Rajan, A.C., Tran, H., Chen, L., Kim, C., Ramprasad, R.: Polymer informatics with multi-task learning. Patterns **2**(4) (2021)

[11] Dinh, T., Zeng, Y., Zhang, R., Lin, Z., Gira, M., Rajput, S., Sohn, J.-y., Papailiopoulos, D., Lee, K.: Lift: Language-interfaced fine-tuning for non-language machine learning tasks. Advances in Neural Information Processing Systems **35**, 11763–11784 (2022)

[12] Touvron, H., Lavril, T., Izacard, G., Martinet, X., Lachaux, M.-A., Lacroix, T., Rozière, B., Goyal, N., Hambro, E., Azhar, F., et al.: Llama: Open and efficient foundation language models. arXiv preprint arXiv:2302.13971 (2023)

[13] Achiam, J., Adler, S., Agarwal, S., Ahmad, L., Akkaya, I., Aleman, F.L., Almeida, D., Altenschmidt, J., Altman, S., Anadkat, S., et al.: Gpt-4 technical report. arXiv preprint arXiv:2303.08774 (2023)

[14] Zeng, Z., Yu, J., Gao, T., Meng, Y., Goyal, T., Chen, D.: Evaluating large language models at evaluating instruction following. Preprint at https://arxiv.org/abs/2310.07641 (2023)

[15] Wilkinson, M.D., Dumontier, M., Aalbersberg, I.J., Appleton, G., Axton, M., Baak, A., Blomberg, N., Boiten, J.-W., da Silva Santos, L.B., Bourne, P.E., Bouwman, J., Brookes, A.J., Clark, T., Crosas, M., Dillo, I., Dumon, O., Edmunds, S., Evelo, C.T., Finkers, R., Gonzalez-Beltran, A., Gray, A.J.G., Groth, P., Goble, C., Grethe, J.S., Heringa, J., 't Hoen, P.A.C., Hooft, R., Kuhn, T., Kok, R., Kok, J., Lusher, S.J., Martone, M.E., Mons, A., Packer, A.L., Persson, B., Rocca-Serra, P., Roos, M., Schaik, R., Sansone, S.-A., Schultes, E., Sengstag, T., Slater, T., Strawn, G., Swertz, M.A., Thompson, M., Lei, J., Mulligen, E., Velterop, J., Waagmeester, A., Wittenburg, P., Wolstencroft, K., Zhao, J., Mons, B.: The FAIR Guiding Principles for scientific data management and stewardship. Scientific Data **3**(1), 160018 (2016) https://doi.org/10.1038/sdata.2016.18

[16] Scheffler, M., Aeschlimann, M., Albrecht, M., Bereau, T., Bungartz, H.-J., Felser, C., Greiner, M., Groß, A., Koch, C.T., Kremer, K., *et al.*: Fair data enabling new

horizons for materials research. Nature **604**(7907), 635–642 (2022)

[17] Xu, Z., Jain, S., Kankanhalli, M.: Hallucination is inevitable: An innate limitation of large language models. Preprint at https://arxiv.org/abs/2401.11817 (2024)

[18] Dunn, A., Wang, Q., Ganose, A., Dopp, D., Jain, A.: Benchmarking materials property prediction methods: the matbench test set and automatminer reference algorithm. npj Computational Materials **6**(1), 138 (2020)

[19] Chen, Y., Qian, S., Tang, H., Lai, X., Liu, Z., Han, S., Jia, J.: LongLoRA: Efficient Fine-tuning of Long-Context Large Language Models (2023)

[20] Dao, T.: FlashAttention-2: Faster Attention with Better Parallelism and Work Partitioning (2023)

[21] Rasley, J., Rajbhandari, S., Ruwase, O., He, Y.: DeepSpeed: System optimizations enable training deep learning models with over 100 billion parameters. In: Proceedings of the 26th ACM SIGKDD International Conference on Knowledge Discovery & Data Mining, pp. 3505–3506 (2020). https://doi.org/10.1145/3394486.3406703

[22] Kawazoe, Y., Yu, J.-Z., Tsai, A.-P., Masumoto, T.: Nonequilibrium phase diagrams of ternary amorphous alloys. Springer (1997)

[23] Pei, Z., Yin, J., Hawk, J.A., Alman, D.E., Gao, M.C.: Machine-learning informed prediction of high-entropy solid solution formation: Beyond the hume-rothery rules. npj Computational Materials **6**(1), 50 (2020)

[24] Batra, R., Chen, C., Evans, T.G., Walton, K.S., Ramprasad, R.: Prediction of water stability of metal–organic frameworks using machine learning. Nature Machine Intelligence **2**(11), 704–710 (2020)

[25] Beard, E.J., Sivaraman, G., Vázquez-Mayagoitia, Á., Vishwanath, V., Cole, J.M.: Comparative dataset of experimental and computational attributes of uv/vis absorption spectra. Scientific data **6**(1), 307 (2019)

[26] Nagasawa, S., Al-Naamani, E., Saeki, A.: Computer-aided screening of conjugated polymers for organic solar cell: classification by random forest. The Journal of Physical Chemistry Letters **9**(10), 2639–2646 (2018)

[27] Gaulton, A., Bellis, L.J., Bento, A.P., Chambers, J., Davies, M., Hersey, A., Light, Y., McGlinchey, S., Michalovich, D., Al-Lazikani, B.: Chembl: a large-scale bioactivity database for drug discovery. Nucleic acids research **40**(D1), 1100–1107 (2012)

[28] Moosavi, S.M., Nandy, A., Jablonka, K.M., Ongari, D., Janet, J.P., Boyd, P.G., Lee, Y., Smit, B., Kulik, H.J.: Understanding the diversity of the metal-organic

framework ecosystem. Nature communications **11**(1), 1–10 (2020)

[29] Chung, Y., Haldoupis, E., Bucior, B., Haranczyk, M., Lee, S., Vogiatzis, K., Ling, S., Milisavljevic, M., Zhang, H., Camp, J., et al.: Computation-Ready Experimental Metal-Organic Framework (CoRE MOF) 2019 Dataset. Zenodo https://doi.org/10.5281/zenodo (2019)

[30] Moosavi, S.M., Novotny, B.Á., Ongari, D., Moubarak, E., Asgari, M., Kadioglu, Ö., Charalambous, C., Ortega-Guerrero, A., Farmahini, A.H., Sarkisov, L., *et al.*: A data-science approach to predict the heat capacity of nanoporous materials. Nature materials **21**(12), 1419–1425 (2022)

[31] Mobley, D.L., Guthrie, J.P.: Freesolv: a database of experimental and calculated hydration free energies, with input files. Journal of computer-aided molecular design **28**, 711–720 (2014)

[32] Griffiths, R.-R., Greenfield, J.L., Thawani, A.R., Jamasb, A.R., Moss, H.B., Bourached, A., Jones, P., McCorkindale, W., Aldrick, A.A., Fuchter, M.J., *et al.*: Data-driven discovery of molecular photoswitches with multioutput gaussian processes. Chemical Science **13**(45), 13541–13551 (2022)

[33] Stanev, V., Oses, C., Kusne, A.G., Rodriguez, E., Paglione, J., Curtarolo, S., Takeuchi, I.: Machine learning modeling of superconducting critical temperature. npj Computational Materials **4**(1), 29 (2018)

[34] Materials Science, M.I.S.: SuperCon. http://supercon.nims.go.jp/index_en.html (2011)

[35] Gaultois, M.W., Sparks, T.D., Borg, C.K., Seshadri, R., Bonificio, W.D., Clarke, D.R.: Data-driven review of thermoelectric materials: performance and resource considerations. Chemistry of Materials **25**(15), 2911–2920 (2013)

[36] Na, G.S., Chang, H.: A public database of thermoelectric materials and system-identified material representation for data-driven discovery. npj Computational Materials **8**(1), 214 (2022)

[37] Huang, D., Cole, J.M.: A database of thermally activated delayed fluorescent molecules auto-generated from scientific literature with chemdataextractor. Scientific Data **11**(1), 80 (2024)

[38] Zhao, J., Cole, J.M.: A database of refractive indices and dielectric constants auto-generated using chemdataextractor. Scientific data **9**(1), 192 (2022)

[39] Zhuo, Y., Mansouri Tehrani, A., Brgoch, J.: Predicting the band gaps of inorganic solids by machine learning. The journal of physical chemistry letters **9**(7), 1668–1673 (2018)

[40] Dong, Q., Cole, J.M.: Auto-generated database of semiconductor band gaps using chemdataextractor. Scientific Data **9**(1), 193 (2022)

[41] Isert, C., Atz, K., Jiménez-Luna, J., Schneider, G.: Qmugs, quantum mechanical properties of drug-like molecules. Scientific Data **9**(1), 273 (2022)

[42] Delaney, J.S.: Esol: estimating aqueous solubility directly from molecular structure. Journal of chemical information and computer sciences **44**(3), 1000–1005 (2004)

[43] McDonagh, J.L., Nath, N., De Ferrari, L., Van Mourik, T., Mitchell, J.B.: Uniting cheminformatics and chemical theory to predict the intrinsic aqueous solubility of crystalline druglike molecules. Journal of chemical information and modeling **54**(3), 844–856 (2014)